https://dx.doi.org/10.4314/dujopas.v11i1a.26
ISSN (Print): 2476-8316
ISSN (Online): 2635-3490
Dutse Journal of Pure and Applied Sciences (DUJOPAS), *Vol. 11 No. 1a March 2025*

Aminoantipyrine-derived Schiff Bases containing Thiophenyl, Furanyl / Isatin nucleus: Antioxidant Study, DFT and Molecular Docking Profile

Abdullahi Owolabi Sobola[1, 2]*, Olarewaju Rafiu Shaibu[3], Oluwafemi Segun Aina[3], David Asuquo Ante[1], Ayemu Adeniyi Adejare [1], Felicia Oluwafunmilayo Orungbamila[1], Benice Prosper Ajuebor [1], Barakat Oluwakoyinsola Raji[1], Omoniyi Olayinka Onifade[4], Saliu Alao Amolegbe [5]

[1]Department of Chemistry,
Faculty of Science,
Lagos State University,
Ojo,
Lagos,
Nigeria.

[2]Afrıcan Centre of Excellence for Innovative and Transformative STEM Education (ACEITSE),
Lagos State University,
Ojo,
Lagos,
Nigeria.

[3]Department of Chemistry,
Faculty of Science,
University of Lagos,
Akoka,
Lagos,
Nigeria.

[4]Department of Biochemistry,
Faculty of Basic Medical Sciences,
College of Medicine,
University of Lagos,
Idi-Araba,
Lagos,
Nigeria.

[5]Department of Pure and Applied Chemistry,
College of Physical Sciences,
Federal University of Agriculture,
Abeokuta,
Ogun State,
Nigeria.

Email: abdullahi.sobola@lasu.edu.ng

**Author for Correspondence*

Abstract

This study presents the antioxidant and in-silico profiling of molecular interactions of a series of aminoantipyrine-derived Schiff bases (L_1-L_6). Compounds L_1-L_3 contains the thiophenyl or furanyl moiety while compounds L_4-L_6 were obtained from isatin or its derivatives. The antioxidant activity of the compounds is dose-dependent and is strongly correlated to the concentrations of the samples. The optimized geometries and the electronic properties of the compounds were obtained using density functional theory (DFT) B3LYP hybrid functional with 631+6(d,p) basis set. All the compounds were docked into the binding sites of cytochrome oxidase (PDB ID: 3mk7), myeloperoxidase (PDB ID: 6wy7), NADPH oxidase (PDB ID: 8wej) and xanthine oxidase (PDB ID: 1fiq) proteins. The isatin-based compounds exhibited higher free radical scavenging ability and higher binding affinity than the thiophenyl or furanyl analogues.

Keywords: Free radicals, Aminoantipyrine, Isatin, Molecular electrostatic potential, chemical reactivity

INTRODUCTION

Reactive oxygen species are generated during various biochemical processes and the inability of the body to effectively detoxify itself of these reactive species is called oxidative stress (Ito *et al*., 2019). Various degenerative disease conditions have been linked to the incidence of these toxic reactive species (Abuja and Albertini, 2001). Anti-oxidants, which could be from natural or synthetic sources, help to reduce the effect of reactive species on normal physiological functions in human. Specifically, the anti-oxidant activity of bioactive compounds is manifested through peroxides decomposition or scavenging of free radicals. Other mechanisms include limiting further abstraction of hydrogen and chain initiation (Joseph *et al*., 2013).

Reactive oxygen species include superoxide (O_2^-), hydrogen peroxide (H_2O_2), hydroxyl radicals ($OH\cdot$) and singlet oxygen ($^1O_2$) (Kostova and Saso, 2013). Superoxide and hydrogen peroxide are produced in the biological systems through partial reduction of molecular oxygen while hydroxyl radical is generated through one-electron reduction of hydrogen peroxide (Kostova and Saso, 2013). Furthermore, the reaction of reactive oxygen species (ROS) with biological molecules produces several other reactive species such as polyunsaturated lipids, thiols, and nitric oxide. The presence of excessive nitric oxide radical in biological system is undesirable because they are easily converted to more reactive species such as nitric dioxide and peroxynitrite in the presence of oxygen or superoxide (Abuja and Albertini, 2001). Similarly, hydrogen peroxide, though less reactive is converted to the highly reactive hydroxyl radical in the presence of metal ions. The hydroxyl radical is highly involved in the oxidation of polyunsaturated fatty acids (PUFA) such as arachidonic and linoleic acids (Angelova et al., 2021). In addition, such free radical induced lipid peroxidation produces several bioactive aldehydes such as malondialdehyde (MDA) and acroleins (Hodges *et al*., 1999, Roesslein *et al*., 2013). These aldehydes form covalent bond with cellular proteins thereby altering cell functions in the organisms. MDA forms dihydropyridine (DHP) type adducts in the presence of protein-bound lysine residues.

From the foregoing, it is evident that various free radical species are responsible for the incidence of oxidative stress and therefore multiple antioxidant bioassays would be required to evaluate the potency of promising antioxidant agents. In addition, the effect of structural variation on the mode of action of bioactive compounds cannot be overemphasised. Five-

membered heterocyclic compounds constitute the main pharmacophore of most drug agents. For instance, pyrrole is a component of tryptophan, while vitamin C and vitamin B complex contain the furanyl and thiophenyl derivative moieties respectively. Similarly, the report on the pharmacological importance of pyrazolones is well documented (Bekhit *et al*., 2010, Küçükgüzel and Şenkardeş, 2015, Hampp *et al*., 2008, Steinbach *et al*., 2000, Uslaner *et al*., 2009). Consequently, series of aminoantipyrne-based compounds have been synthesised and evaluated for various pharmacological activity as anti-tumour, anti-inflammatory, antimicrobial, antioxidant and antifungal agents (Sakthivel *et al*., 2020, Mohanram and Meshram, 2014, Joseph *et al*., 2013).

Nonetheless, there is a dire need to understand the molecular interactions of these compounds with amino acid residues at the binding sites of target antioxidant proteins. The understanding of molecular interactions is a vital step in drug design in the search for an effective and robust drug agent. In-silico molecular docking study is used to predict the binding affinity and nature of different nonbonding interactions within the ligand-protein complexes at the binding sites of target proteins (Rana *et al*., 2021, Yadav *et al*., 2017, Ponnan *et al*., 2013). Similarly, the values of quantum mechanical electronic parameters obtained from DFT theoretical calculations are suggestive of the chemical reactivity of potential drug agents (Ovung and Bhattacharyya, 2021, Reddy *et al*., 2016).

In this study, therefore, we evaluated the free radical scavenging ability and comparative in-silico molecular binding interactions of a series of aminoantipyrine Schiff bases containing the thiophenyl, furanyl or isatin moiety as potential inhibitors of target antioxidant proteins viz: cytochrome oxidase (PDB ID: 3mk7), myeloperoxidase (PDB ID: 6wy7), NADPH oxidase (PDB ID: 8wej) and xanthine oxidase (PDB ID: 1fiq) proteins.

METHODOLOGY

Materials

The chemicals and reagents used for the synthesis of the Schiff bases were of reagent grade and needed no further purification. They were obtained from Sigma Aldrich. The NMR spectra of compounds L_1 – L_6 were recorded in $CDCl_3$ with TMS as internal standard on Bruker Avance 500MHz spectrometer for ^1H and 126MHz for ^{13}C at 27 °C. The infrared spectra were recorded using a Bruker TENSOR 27 single channel infrared spectrometer. The elemental analysis, CHNS, of the compounds was done using Vario EL cube model elemental analyser while the melting points were determined using Griffin melting point apparatus.

Synthesis of the Aminoantipyrine-derived Schiff bases, L_1 –L_6

The Schiff base compounds, L_1 – L_6 (2-thiophenyl, 3-methyl-2-thiophenyl, furfuryl, NO_2-isatin, Br-isatin and isatin moieties) were synthesized according to the general synthetic procedure in the literature (Emami *et al*., 2022, Sakthivel *et al*., 2020, Sherif *et al*., 2021, Agarwal and Agarwal, 2001). The analytical data for the compounds are presented in Table 1 while the spectral data are presented as supplementary material. The spectroscopic properties of the compounds have earlier been reported (Agarwal and Agarwal, 2001, Al-Saif, 2013, Joseph and Rani, 2014, Vinodkumar and Radhakrishnan, 1997, Hu *et al*., 2022). The structures for the aminoantipyrine Schiff bases are presented in Figures 1 and 2.

Table 1: Physical and Analytical Data for the Aminoantipyrine Schiff Bases, L_1 – L_6

Compds	Molecular Formula	Colour	%Yield	M.Pt (°C)	Found (Calculated) %C	%H	%N	%S
L_1	$C_{16}H_{15}N_3OS$	Yellow	91	148-150	64.73 (64.62)	4.92 (5.08)	14.10 (14.13)	10.72 (10.78)
L_2	$C_{17}H_{17}N_3OS$	Brown	81	152-154	65.75 (65.56)	5.31 (5.50)	13.44 (13.49)	10.40 (10.30)
L_3	$C_{16}H_{15}N_3O_2$	Yellow	92	188-190	68.32 (68.13)	5.24 (5.37)	14.80 (14.90)	----
L_4	$C_{19}H_{15}N_5O_4$	Orange	89.12	>250	60.39 (60.47)	3.55 (4.01)	18.51 (18.56)	----
L_5	$C_{19}H_{15}N_4O_2Br$	Orange	72.53	240-242	54.99 (55.49)	3.20 (3.67)	13.30 (13.62)	-----
L_6	$C_{19}H_{16}N_4O_2$	Brick-red	68.75	139-140	68.90 (68.66)	4.64 (4.85)	16.76 (16.86)	-----

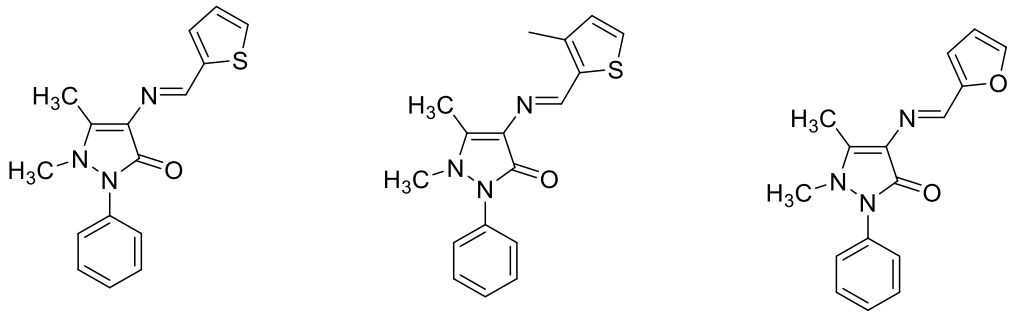

L_1 L_2 L_3

Figure 1: Aminoantipyrine-derived Schiff bases with thiophenyl / furfuryl moiety, L_1 - L_3. Aminoantipyrine was condensed with thiophene-2-carboxaldehyde, 3-methyl-thiophene-2-carboxaldehyde or furan-2-carboxaldehyde (furfural) to obatain compounds L_1, L_2 and L_3 respectively.

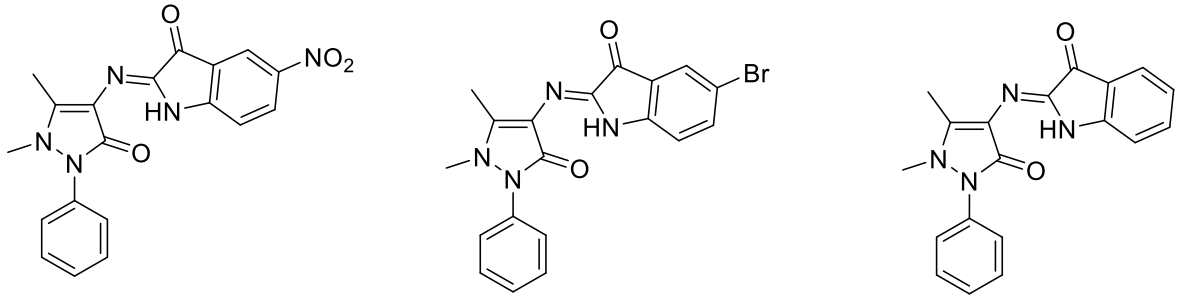

L_4 L_5 L_6

Figure 2: Aminoantipyrine-derived Schiff base ligands containing the isatin moiety, L_4 - L_6. Aminoantipyrine was condensed with nitro-isatin, bromo-isatin,or isatin, to obatain compounds L_4, L_5 and L_6 respectively.

Antioxidant Study of the Schiff Bases

The Schiff bases were evaluated for their potential antioxidant activity by determining their ability to scavenge DPPH (1,1'-diphenyl-2-picryl-hydrazil), nitric oxide and hydrogen peroxide free radicals. The lipid peroxidation inhibition ability of the compounds was also determined.

The DPPH free radical scavenging activity was determined by Blois method (Kedare and Singh, 2011) using 1,1'-diphenyl-2-picryl-hydrazil. The reference antioxidant was ascorbic acid (Vit. C), while the samples were prepared at concentration range of 25 – 100 µg/mL. The

assay was carried out in duplicate and the mean values of the absorbance were used to calculate the percentage radical scavenging activity of the compounds as expressed in equation 1:

$$\%\, Scavenging \cdots activity = \frac{Absorbance \cdots Control - Absorbance \cdots Sample}{Absorbance \cdots Control} \times 100 \cdots\cdots (1)$$

On the other hand, the nitric oxide scavenging activity of the Schiff base ligands was measured by Griess reaction (Ali *et al*., 2020) using sodium nitroprusside solution while the Ruch method (Ruch *et al*., 1989) was used to evaluate the ability of the compounds to scavenge hydrogen peroxide free radicals. Similarly, the lipid peroxide inhibition ability of the compounds was assessed by the reaction of thiobarbituric acid (TBA) with malondialdehyde (MDA) to give thiobarbituric reactive substances which was measured by colorimetry method at 540 nm (Ito *et al*., 2019, Ohkawa *et al*., 1979). All the assays were carried out in duplicate and the percentage of free radicals inhibition of the compounds was calculated as expressed in equation 1.

Statistical Analysis

The IC_{50} values for the compounds were calculated from the regression equations obtained from Microsoft excel using the mean values for the percentage radical scavenging activity. The two-way ANOVA for the percentage radical inhibition was done using Graph pad Prism 5.

DFT Study

The theoretical calculations for the compounds were done on Gaussian 09W software package. The optimized geometry, vibrational frequencies, frontier molecular orbitals, molecular electrostatic potential (MEP) contour maps and the quantum mechanical electronic properties of the molecules were obtained using Becke's three parameters hybrid exchange correlation functional (B3LYP) with 6-31+G(d,p) basis set (Lee *et al*., 1988, Becke, 1993). The electronic properties were determined for the compounds using time-dependent density functional theory (TD-DFT) level in ethanol or methanol.

Docking Study

The six aminoantipyrine derived Schiff bases were subjected to docking studies for binding affinity and non-bonding molecular interactions evaluation using PyRx AutoDock Vina wizard (Eberhardt *et al*., 2021). The crystal structures of the target protein molecules were downloaded from the protein data bank at rcsb.org (https://www.rcsb.org/) with 3.20, 2.90, 2.79 and 2.50 Å resolutions for cytochrome oxidase (PDB ID: 3mk7), myeloperoxidase (PDB ID: 6wy7), NADPH oxidase (PDB ID: 8wej) and xanthine oxidase (PDB ID: 1fiq) respectively. The structures were obtained in the .pdb format and subsequently processed using BIOVIA Discovery Studio (DS) 2021 Visualizer (https://discover.3ds.com/discovery-studio-visualizer-download) to eliminate unwanted ligands, heteroatoms and water molecules. In addition, polar hydrogen atoms were added to the structure as required. The protein molecules and the synthesized compounds were converted to Autodock format, and a flexible ligand to rigid protein approach was employed.

All possible binding sites on the target protein were explored during the docking process. The docking calculations were performed within a cubic grid range of dimensions 90 × 75 × 90 centered on the protein, encompassing the entire protein structure. A grid spacing of 1.00 Å was utilized to generate the grid maps using the autogrid module of AutoDock tools. Each ligand underwent nine independent runs to ensure accuracy. Potential binding sites were identified and energetically favourable binding conformations were elected using Autodock

Vina (Eberhardt *et al*., 2021). The binding modes, along with their respective binding affinities and RSB (upper and lower) values, were obtained to guide the selection of the highest scoring binding conformation for each ligand. The binding mode with the best binding affinity was chosen. The ligand-protein complexes were analyzed using DS Visualizer.

RESULTS AND DISCUSSION

The antioxidant activity of the aminoantipyrine-derived Schiff bases (L_1 –L_6) has been determined using DPPH, nitric oxide and hydrogen peroxide free radicals scavenging activity as well as lipid peroxidation inhibition activity.

The standard antioxidant agent used for the study was ascorbic acid (vitamin C). The anti-oxidant activity of the aminoantipyrine Schiff bases is illustrated in Figure 3 as IC_{50} values in mg/L. The DPPH bioassay revealed that the Schiff bases containing the isatin nucleus (L_4 – L_6) exhibited higher activity than the thiophenyl and furanyl nucleus (L_1, L_2 and L_3). In addition, the presence of a nitro group in L_4 significantly reduces ($p < 0.001$) the DPPH radical scavenging ability of the isatin Schiff base, L_6, with IC_{50} values of 50.01 mg/L and 35.18 mg/L for L_4 and L_6 respectively. Similar effect was observed for the NO, H_2O_2 and lipid peroxide bioassay studies (Figure 3). The free radical scavenging activity of the compounds is concentration dependent as shown in the supplementary data / S19. The antioxidant activity of L_6 against NO and H_2O_2 as well as lipid peroxidation is significantly higher than the anti-oxidant activity of vitamin C. Similarly, the radical scavenging ability of the 2-methyl-thiophenyl analogue, L_2, against DPPH and hydrogen peroxide free radicals was observed to be significantly, at $p < 0.001$, higher than the inhibition produced by compounds L_1 and L_3.

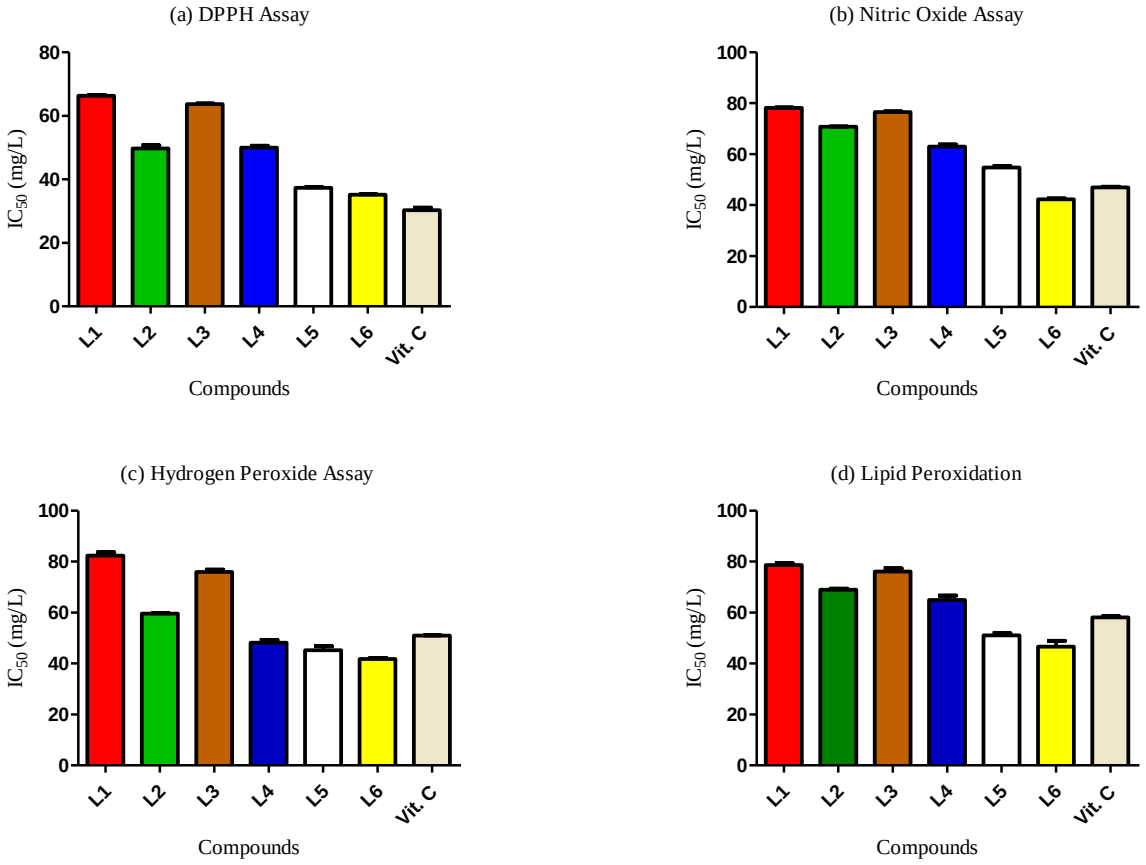

Figure 3: Anti-oxidant activity for the aminoantipyrine Schiff bases, L_1 – L_6. The half-maximal inhibitory concentrations (IC_{50}) of the compounds are expressed as mg/mL for the (a) DPPH (b) Nitric oxide (c) Hydrogen peroxide and, (d) lipid peroxidation assays.

DFT Study

The optimized geometries for the compounds presented in the supplementary data / S20 were obtained using DFT theory with B3LYP basis set and the quantum mechanical electronic properties are presented in Table 2. Parameters such as the highest occupied molecular orbital (HOMO), lowest unoccupied molecular orbital (LUMO) energies, the HOMO-LUMO energy gap (E), global hardness (η) and softness (S), as well as the electron affinity (A) of the compounds were determined. The values of the ionization potential (I), electrophilicity (ω), chemical potential (μ) and the dipole moment of the compounds were equally calculated.

The energies of the highest occupied molecular orbital and the lowest occupied molecular orbital are related to the ionization potential and the electron affinity of molecules according to the Koopman's theory (Reddy *et al*., 2016) as illustrated in equations 2 and 3. In addition, the kinetic stability and chemical reactivity of conjugated systems could be inferred from the energy gap between the HOMO-LUMO orbitals. A low HOMO-LUMO energy difference indicates low kinetic stability and high chemical reactivity (Rana *et al*., 2021).

$$A = -E_{LUMO} \quad \text{---------- } 2$$

$$I = -E_{HOMO} \quad \text{---------- } 3$$

The HOMO-LUMO energy gap calculated for the isatin-derived Schiff bases, L_4 – L_6, is smaller compared with the thiophenyl or furanyl analogues. This suggests higher chemical reactivity and low kinetic stability (Ovung and Bhattacharyya, 2021) for compounds L_4 – L_6. Similarly, global hardness and softness have been used to predict the chemical reactivity of conjugated molecules. Global hardness is calculated as:

$$\eta = \frac{\Delta E}{2} \quad \text{---------- } 4$$

Low global hardness corresponds to high kinetic stability and low reactivity. The isatin-based compounds have lower global hardness (1.515 – 1.495 eV) than the thiophenyl or furanyl analogues (1.962 – 1.893 eV). Softness is expressed as the reciprocal of hardness. High values of global softness indicate higher chemical reactivity for the isatin based compounds (Hoque *et al*., 2018). Similarly, the values of electronegativity (χ) obtained from the DFT calculations are related to the chemical potential (μ) of the molecules as illustrated in equation 5. The isatin-based compounds have higher chemical potentials and are expected to be more reactive than the thiophenyl or furanyl analogues. In addition, the chemical reactivity of the compounds is also defined by high electrophilicity index (Mohamed *et al*., 2021) and dipole moment values as indicated in Table 2. The electrophilicity index of the isatin-based compounds (L_4 –L_6) is higher than those of the thiophenyl and furanyl based compounds (L_4 –L_6). It was also observed that the presence of the electronegative groups (Br or NO_2) enhanced the elecrophilicity of compounds L_4 and L_5 with electrophilicity values of 2.349 and 2.112 eV respectively.

$$\mu = -\chi \quad \text{---------- } 5$$

Table 2: Electronic Properties of the Compounds.

(eV)	L_1	L_2	L_3	L_4	L_5	L_6
HOMO	-5.450	-5.395	-5.394	-5.645	-5.432	-5.374
LUMO	-1.664	-1.591	-1.470	-2.655	-2.492	-2.344
ΔE	3.787	3.804	3.924	2.989	2.940	3.030
I	5.450	5.395	5.394	5.645	5.432	5.374
A	1.664	1.591	1.470	2.655	2.492	2.344
χ	3.560	3.490	3.430	4.150	3.960	3.860
μ	-3.560	-3.490	-3.430	-4.150	-3.960	-3.860
η	1.893	1.902	1.962	1.495	1.470	1.515
S	0.528	0.526	0.510	0.669	0.680	0.660
Ω	0.731	0.665	0.551	2.349	2.112	1.813
Dipole moment (debye)	5.240	4.455	4.945	18.048	12.070	8.928

The plots of the frontier molecular orbitals (Figures 4, supplementary data / S21 and S22) for the compounds revealed that the electron density are localized on the thiophenyl (L_1, L_2), furanyl (L_3) or the isatin (L_4 – L_6) moiety and extend only unto the pyrazolonyl scaffolds of the amioantypyrine moiety excluding the phenyl group.

Furthermore, an insight into the molecular recognition at the surface of the compounds was achieved by studying the molecular electrostatic contour maps (MEP) obtained from the DFT theory B3LYP hybrid functional with 6-31+G(d,p) basis set. MEP describes the distribution of electron density within the surface of the compounds and helps to recognize the reactive sites responsible for biological reactivity at the surface of the molecules (Abraham *et al*., 2019, Rana *et al*., 2021).

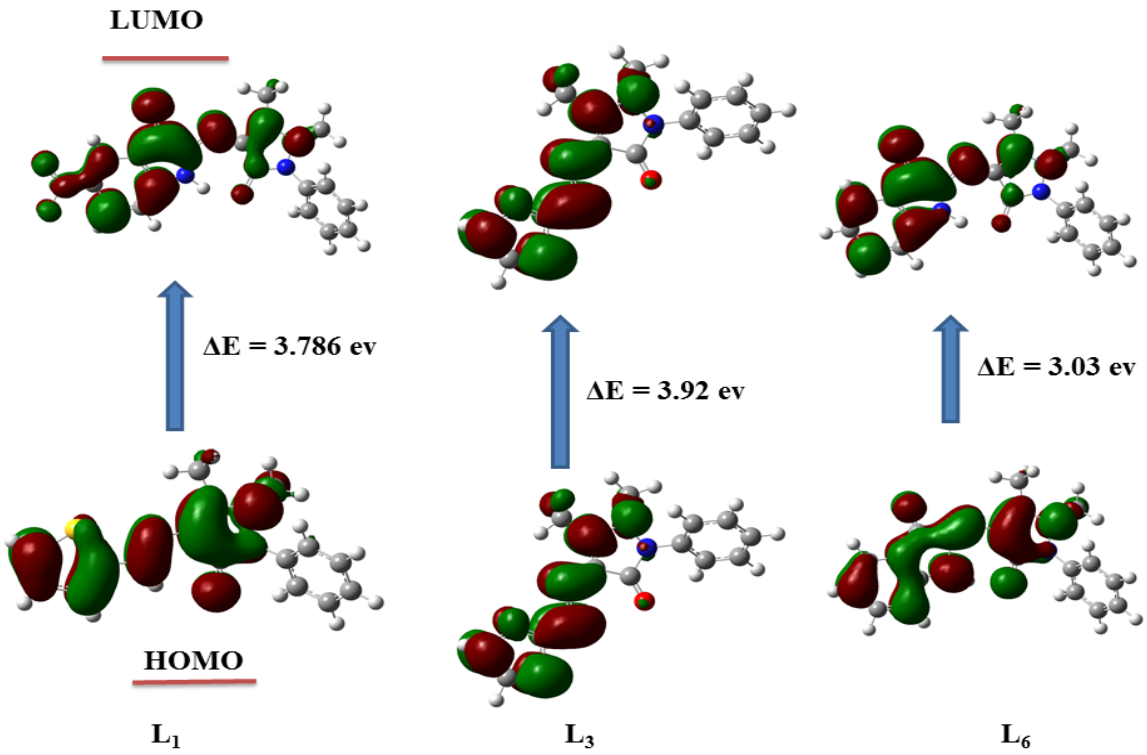

Figure 4: Frontier Molecular Orbitals for the thiophenyl, furanyl and isatin-based compounds, showing the electron density domain and the HOMO-LUMO energy gaps for the compounds L_1 and L_3 and L_6 obtained from thiophene-2-carboxaldehyde, furan-2-carboxaldehyde and, 1H-indole-2,3-dione (isatin) respectively.

The region with the lowest MEP is sensitive to electrophilic attack while nucleophilic attack occurs at the region of highest MEP. The electrostatic potential at the surface of the compounds are represented with varying graded colours with red and blue corresponding to regions with lowest and highest potential respectively (Truhlar, 1981). The MEP maps for the compounds (Figure 5) show that the carbonyl oxygen of the aminoantipyrine, the hetero-oxygen of the furanyl- and the oxygen atoms of the nitro-isatin moieties have the highest molecular potential and as such are the most susceptible to nucleophilic attack. Similarly, the methyl group was observed to be more favourable to electrophilic attack.

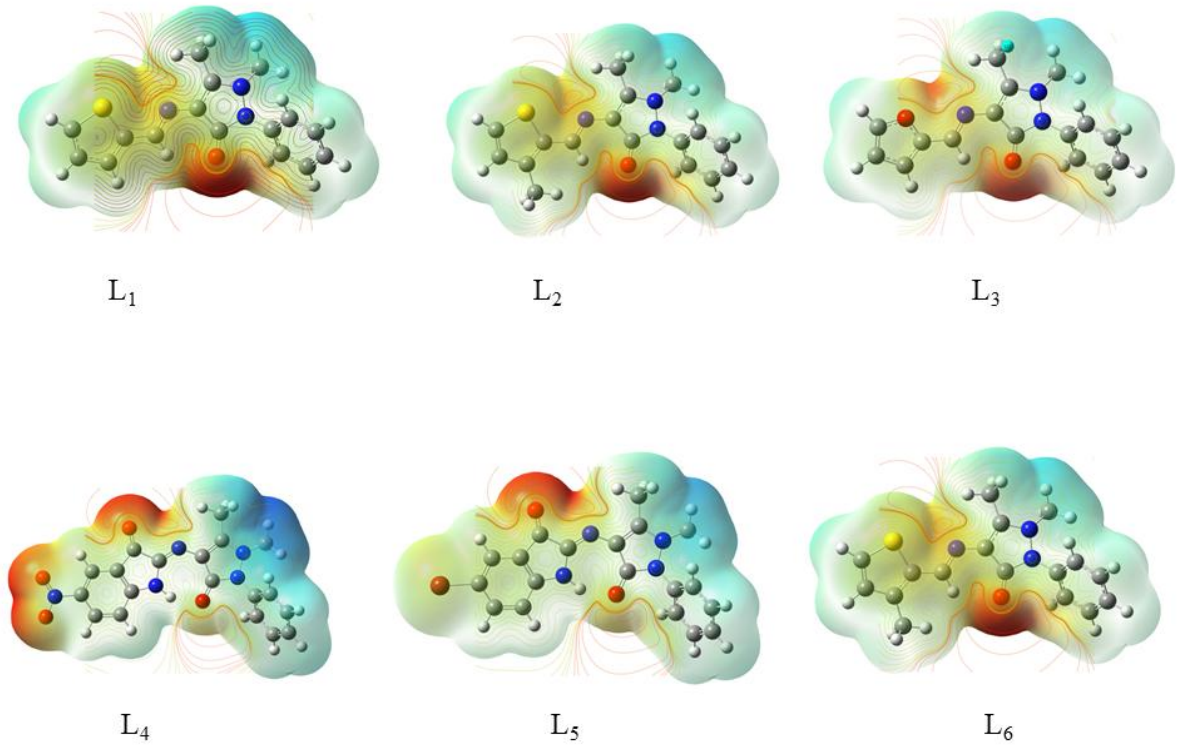

Figure 5: Molecular electrostatic contour maps (MEP) maps for the compounds. The red and blue colours represent regions of strong electrophilic and nucleophilic attacks respectively.

Docking Study

The aminoantipyrine Schiff base compounds were subjected to in-silico docking study in order to understand their binding affinity and non-bonding interactions with amino acid residues at the binding sites of different target antioxidant proteins. The binding energies of the compounds against cytochrome oxidase (PDB ID: 3mk7), myeloperoxidase (PDB ID: 6wy7), NADPH Oxidase (PDB ID: 8wej) and xanthine Oxidase (PDB ID: 1fiq) are presented in Table 3. The binding energies provide an insight into the binding affinities of the compounds with the target proteins. The aminoantipyrine-based ligands exhibit a range of binding affinities across different protein targets, with binding energies denoted in kcal/mol. The docking study showed that the aminoantipyrine Schiff base series containing the isatin nucleus (L_4, L_5 & L_6) have higher negative binding energies and are thus predicted to exhibit higher binding affinity (Rana *et al*., 2021) than either of the thiophenyl (L_1, L_2) or furanyl (L_3) analogues against 1fiq, 3mk7 and 6wy7 proteins. Ligand L_3, however, exhibited the highest binding affinity against the 8wej protein.

Table 3: Binding Energies for the Ligands-Proteins Complexes (kcal/mol)[a].

Ligands	Binding energy			
	1fiq	3mk7	6wy7	8wej
L_1	-6.2	-6.4	-7.3	-5.8
L_2	-6.5	-65	-7.5	-5.7
L_3	-6.5	-6.2	-7.2	-6.8
L_4	-7.5	-8.0	-8.4	-6.7
L_5	-7.2	-7.4	-8.6	-6.5
L_6	-7.7	-7.7	-8.4	-6.4

[a]The binding energies obtained for the interactions of the ligands with the various antioxidant target proteins are expressed in kcal/mol. Compounds L_1-L_6 formed four different complexes with cytochrome oxidase (PDB ID: 3mk7), myeloperoxidase (PDB ID: 6wy7), NADPH Oxidase (PDB ID: 8wej) and xanthine Oxidase (PDB ID: 1fiq) respectively.

Ligands L_6, L_4 and L_5 had the highest binding affinity for 1fiq, 3mk7 and 6wy7 proteins with binding energies of -7.7, -8.0 and -8.6 kcal respectively. The variations in binding affinity across different proteins and ligands reflect the diverse interactions and potential efficacy of the synthesized compounds, highlighting their suitability for further exploration in drug development.

The Schiff base ligands exhibit various non-bonding interactions with different amino acid residues at the binding site of the proteins. The binding of ligands L_6 and L_5 was predicted to occur through interactions with both the hydrophobic (PHE, LEU and, ILE) and polar uncharged (ASN and GLN) residues at the binding sites of 1f1q and 6wy7 respectively. On the other hand, the ligand-protein interactions for the L_4-3mk7 and L_3-8wej complexes were achieved through binding with the hydrophobic (PHE, TYR and, LEU) and polar (THR, GLN and, GLU) residues respectively. Hydrophobic interactions through ALA and LYS were also observed for the L_3-8wej protein complex. The presence of hydrophobic interaction at the protein active site enhances the ligand binding affinity and equally results in the formation of a more stable ligand protein complex. The availability of various hydrophobic interactions at the binding interface of the ligand-protein complexes thus suggests higher biological activity. Similarly, the optimization of hydrophobic interaction at the active site of the binding interface of target protein at the expense of hydrogen bonding could elicit improved binding affinity of the ligands (Patil *et al*., 2010).

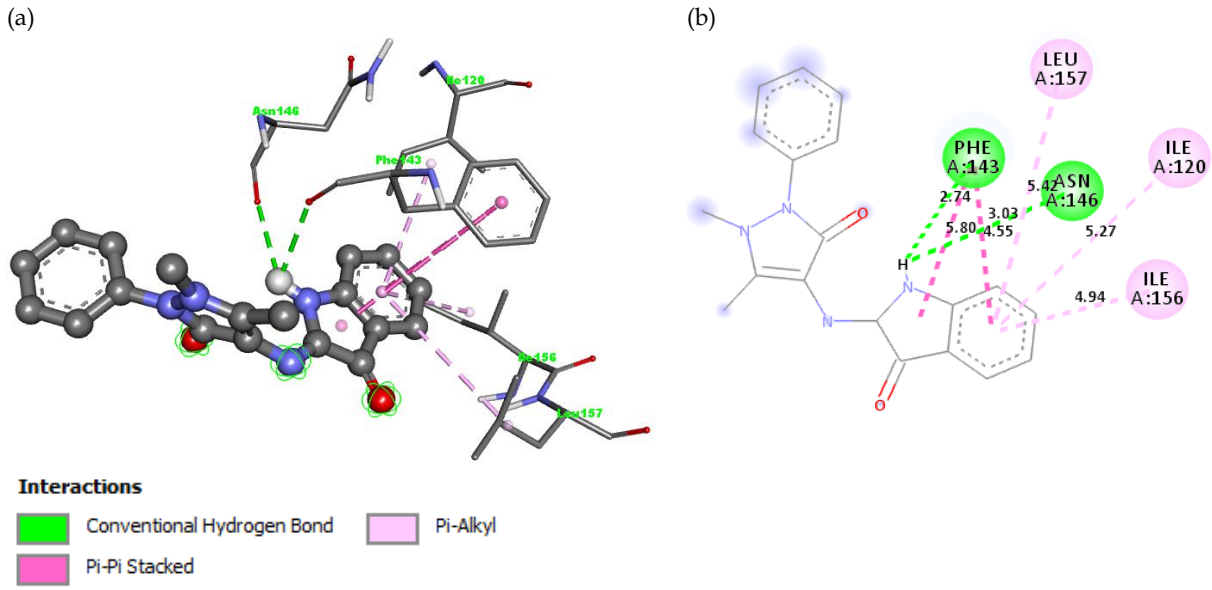

Figure 6: Ligand - protein interactions of L_6-1fiq complex showing the (a) binding residues and (b) bond lengths of interactions at the active site interphase of the protein.

The ligand-protein complex for L_6-1fiq in Figure 6 shows that the structure of compound L_6 was stabilized through two conventional hydrogen bonding interactions with PHE A: 143 and ASN: 146 at a distance of 2.74 and 3.03 Å respectively. The PHE A: 143 residue was equally involved in hydrophobic interaction with a bond length of 5.80 and 4.85 Å. In addition, hydrophobic interactions through pi-pi stacking with LEU A: 157, ILE A: 120 and, ILE A: 156 residues were observed. Hydrogen bonding provides specific interaction of the ligand with the amino acid residues at the active site of the target protein (Glusker, 1998; Kortemme 2003). More importantly it stabilizes the three dimensional architecture of the protein, thereby enhancing the stability of the ligand-protein complex (Panigrahi, 2007). The 3D image of L_6-1fiq complex (supplementary data / S23) displays the solvent-accessible surface (SAS) with areas exposed to the solvent coloured blue. These visualizations demonstrate how hydrophobicity and solvent exposure influence ligand binding, contributing to the stability and interaction dynamics of the ligand-protein complex.

Similarly, hydrophobic nonbonding interaction was responsible for the stabilization of the ligand-protein complex formed between ligand L_4 and 3mk7 protein (Figure 7). The ligand binding was achieved through one conventional hydrogen bond interaction with TYR A: 339 within the binding pocket of the protein while pi-pi and pi-alkyl interactions occur between the ligand's aromatic rings and the side chains of PHE A: 423 and LEU A: 427 residues at a distance of 4.9 and 5.22 Å respectively. The 3D representations of the ligand-protein complex (supplementary data / S23) highlights the hydrophobic (blue) and hydrophilic (brown) regions of the drug-protein complex. These surfaces indicate how the ligand fits into the binding pocket, with hydrophobic areas anchoring the ligand and hydrophilic regions supporting polar interactions. This effectively demonstrates the intricate molecular interactions that secure the ligand within the protein, combining various bonds for a stable binding conformation.

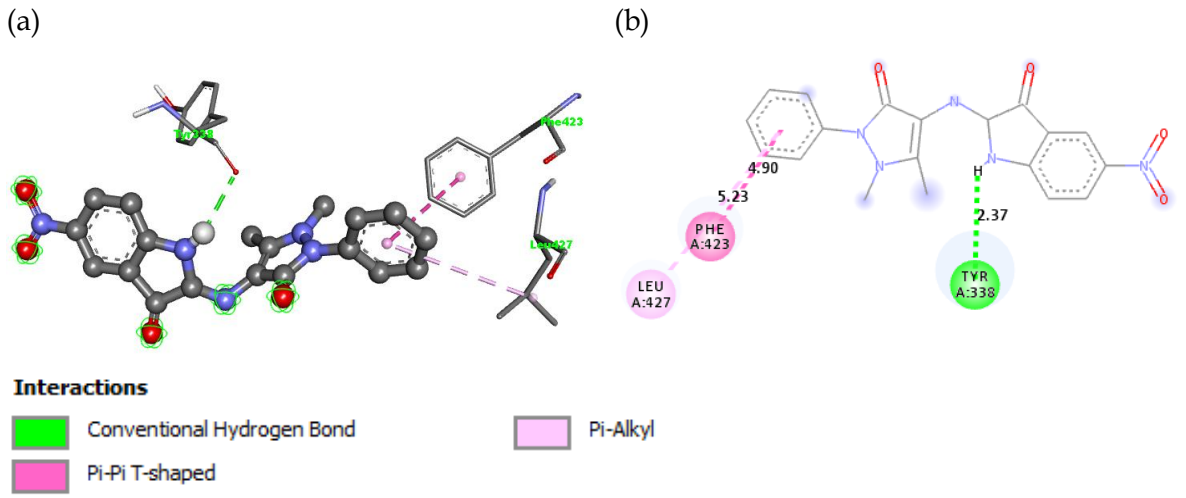

Figure 7: Ligand - protein interactions of L_4 - 3mk7 complex showing the (a) binding residues and (b) bond lengths of interactions at the active site interphase of the protein.

Furthermore, the stabilization of the L_5-6wy7 complex was predicted to occur through nonbonding interactions with polar uncharged (GLN) and hydrophobic (PHE and LEU) residues at the binding site of 6wy7 protein (Figure 8). The nonbonding interaction formed with GLN E: 340 occurred through pi-donor hydrogen bonding at a distance of 3.13 Å while the binding through the PHE E: 552 and LEU E: 361 residues was predicted to result from pi-pi stacked and pi-alkyl interactions respectively. The 3D hydrophobicity surface (brown) of the L_5-6wy7 complex indicates that the ligand is primarily nestled within the hydrophobic regions. Similarly, the solvent accessibility surface (SAS) (blue) shows that part of the ligand is exposed to the solvent, affecting its solubility and stability.

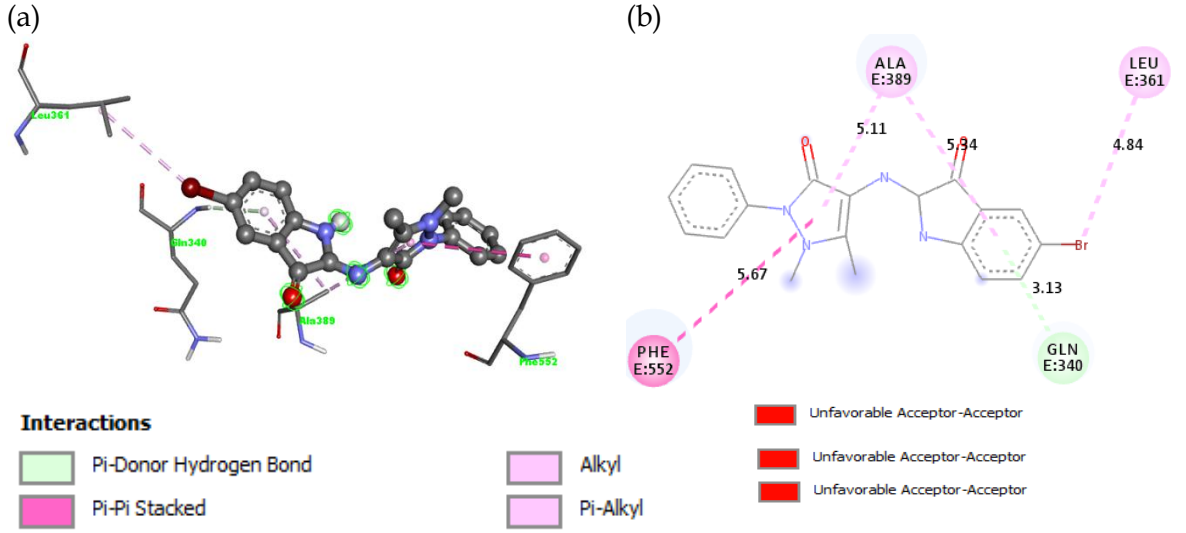

Figure 8: Ligand - protein interactions of L_6-1FIQ complex showing the (a) binding residues and (b) bond lengths of interactions at the active site interphase of the protein.

Nonbonding interactions through polar charged (GLU and ARG) and polar uncharged (THR and GLN) residues were responsible for the stabilization of the L_3-8wej protein complex (Figure 9). One conventional hydrogen bond was formed with THR A: 132 residue at a distance of 2.37 Å while the binding with the GLN: 130 residue occurred through both pi-donor hydrogen and carbon hydrogen bonds. In addition, pi-anion interactions with GLU A: 129 and pi-alkyl interactions with ALA A: 7 contribute to the ligand's positioning and orientation. The ligand's stable conformation was further maintained through pi-sigma

interactions with ARG A: 59 and LYS A: 60 at a distance of 4.90 and 4.58 Å respectively. The 3D structures of the drug-protein complex of ligand L_3 equally shows that the ligand is primarily situated in the hydrophobic regions of the enzyme while the hydrophilic part is exposed to the solvent. This pose is critical for ligand-protein binding, solubility and interaction dynamics.

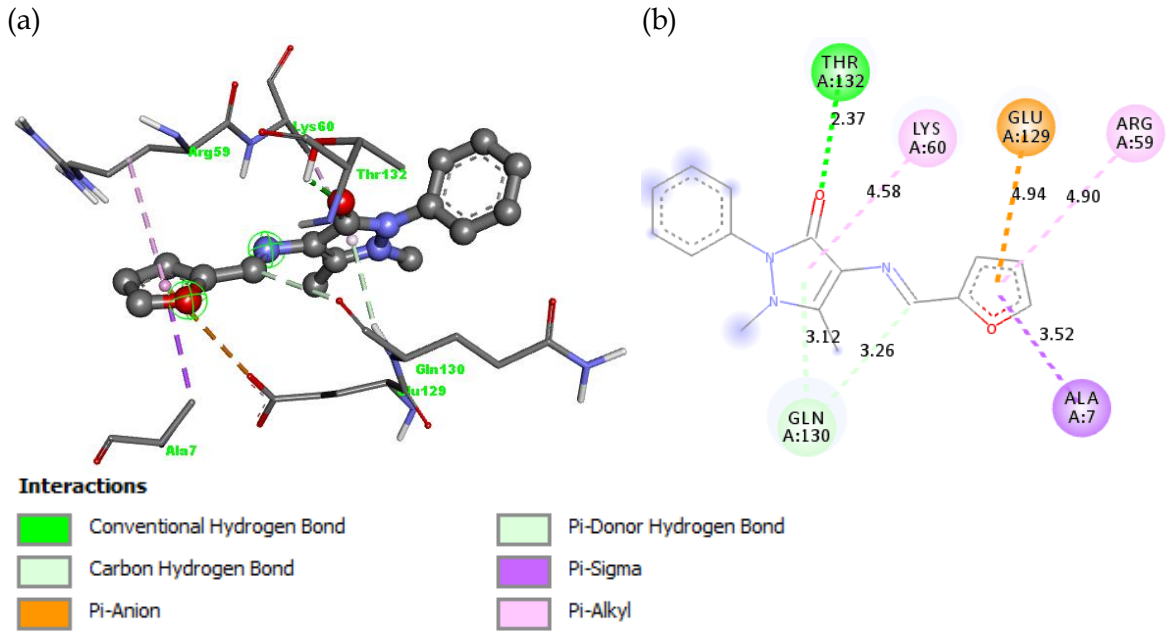

Figure 9: Ligand - protein interactions of L_6-1FIQ complex showing the (a) binding residues and (b) bond lengths of interactions at the active site interphase of the protein.

CONCLUSION

In conclusion, the radical scavenging activity and in-silico molecular interactions of six aminoantipyrine-derived Schiff base compounds (L_1-L_6) containing the thiophenyl, furanyl or isatin moiety have been evaluated. The isatin-based compounds (L_4 – L_6) exhibited higher radical scavenging activity than the thiophenyl and furanyl-based compounds (L_1 - L_3). This was substantiated by the higher chemical reactivity obtained for the isatin based compounds through the DFT calculations. Similarly, higher binding affinity was observed for the isatin-based compounds through in-silico docking study. Specifically, the poses and stabilization of the various ligand–protein complexes occurred through different non-bonding interactions with the residues at the binding sites of the target proteins.

Acknowledgements

We acknowledge the department of chemistry, Lagos State University for providing facilities for this study. In addition, we are very grateful to Rhodes University, South Africa for the opportunity to do the DFT calculations.

Conflict of Interests

The authors declare that there is no conflict of interest in the publication of this manuscript.

REFERENCES

Abraham, C. S., Muthu, S., Prasana, J. C., Armaković, S., Armaković, S. J. and Geoffrey, B. (2019). Computational evaluation of the reactivity and pharmaceutical potential of an organic amine: A DFT, molecular dynamics simulations and molecular docking

approach. *Spectrochimica Acta Part A: Molecular and Biomolecular Spectroscopy,* 222, 117188. https://doi.org/10.1016/j.saa.2019.117188

Abuja, P. M. and Albertini, R. (2001). Methods for monitoring oxidative stress, lipid peroxidation and oxidation resistance of lipoproteins. *Clinica chimica acta,* 306(1-2), 1-17. https://doi.org/10.1016/S0009-8981(01)00393-X

Agarwal, R. K. and Agarwal, H. (2001). The synthesis, structure, and bonding in some lanthanide (III) coordination compounds of 4-[(N-furfural) amino] antipyrine. *Synthesis and Reactivity in Inorganic and Metal-Organic Chemistry,* 31(2), 263-276. https://doi.org/10.1081/SIM-100002046

Al-Saif, F. A. (2013). Spectroscopic, molar conductance and biocidal studies of Pt (IV), Au (III) and Pd (II) chelates of nitrogen and oxygen containing Schiff base derived from 4-amino antipyrine and 2-furaldehyde. *International J.ournal of Electrochemistry Science,* 8(8), 10424-10445. https://doi.org/10.1016/S1452-3981(23)13119-1

Ali, B. M., Boothapandi, M. and Nasar, A. S. (2020). Nitric oxide, DPPH and hydrogen peroxide radical scavenging activity of TEMPO terminated polyurethane dendrimers: Data supporting antioxidant activity of radical dendrimers. *Data in brief,* 28, 104972. https://doi.org/10.1016/j.dib.2019.104972

Angelova, P. R., Esteras, N. and Abramov, A. Y. (2021). Mitochondria and lipid peroxidation in the mechanism of neurodegeneration: Finding ways for prevention. *Medicinal Research Reviews,* 41(2), 770-784. https://doi.org/10.1002/med.21712

Becke, A. D. (1993). Densityfunctional thermochemistry. III. the role of exact exchange. 98 (7): 5648–5652. *The Journal of Chemical Physics.* https://doi. org/10.1063/1.464913

Bekhit, A., A., Hymete, A., Bekhit, E.-D. A., Damtew, A. and Y Aboul-Enein, H. (2010). Pyrazoles as promising scaffold for the synthesis of anti-inflammatory and/or antimicrobial agent: a review. *Mini reviews in medicinal chemistry,* 42(10), 1014-1033. https://doi.org/10.2174/1389557511009011014

Eberhardt, J., Santos-Martins, D., Tillack, A. F. and Forli, S. (2021). AutoDock Vina 1.2. 0: New docking methods, expanded force field, and python bindings. *Journal of chemical information and modeling,* 61, 3891-3898. https://doi.org/10.1021/acs.jcim.1c00203

Emami, L., Khabnadideh, S., Faghih, Z., Solhjoo, A., Malek, S., Mohammadian, A., Divar, M. and Faghih, Z. (2022). Novel n-substituted isatin-ampyrone schiff bases as a new class of antiproliferative agents: Design, synthesis, molecular modeling and in vitro cytotoxic activity. *Journal of Heterocyclic Chemistry,* 59, 1144-1159. https://doi.org/10.1002/jhet.4454

Glusker, J. P. (1998). Directional aspects of intermolecular interactions. In: Weber, E., Aoyama, Y., Caira, M. R., Desiraju, G. R., Glusker, J. P., Hamilton, A. D. *et al*. Design of Organic Solids. Topics in Current Chemistry, Springer, Berlin, Heidelberg. 1 -56. https://doi.org/10.1007/3-540-69178-2_1

Hampp, C., Hartzema, A. G. and Kauf, T. L. (2008). Cost-utility analysis of rimonabant in the treatment of obesity. *Value in Health,* 11, 389-399. https://doi.org/10.1111/j.1524-4733.2007.00281.x

Hodges, D. M., Delong, J. M., Forney, C. F. and Prange, R. K. (1999). Improving the thiobarbituric acid-reactive-substances assay for estimating lipid peroxidation in plant tissues containing anthocyanin and other interfering compounds. *Planta,* 207, 604-611. https://doi.org/10.1007/s004250050524

Hoque, M. J., Ahsan, A. and Hossain, M. B. (2018). Molecular docking, pharmacokinetic, and DFT calculation of naproxen and its degradants. *Biomedical Journal of Scientific & Technical Research,* 9(5), 7360-7365. https://doi.org/10.26717/BJSTR.2018.09.001852

Hu, J., Luo, Y., Hou, M., Qi, J. J., Liang, L. L. and Li, W. G. (2022). Synthesis, structure, and anticancer studies of Cu (II) and Ni (II) complexes based on (5-chlorosalicylaldehyde)-

4-aminoantipyrine Schiff base. *Applied Organometallic Chemistry,* 36(10), e6833. https://doi.org/10.1002/aoc.6833

Ito, F., Sono, Y. and Ito, T. (2019). Measurement and clinical significance of lipid peroxidation as a biomarker of oxidative stress: oxidative stress in diabetes, atherosclerosis, and chronic inflammation. *Antioxidants,* 8(3), 72. https://doi.org/10.3390/antiox8030072

Joseph, J., Nagashri, K. and Rani, G. A. B. (2013). Synthesis, characterization and antimicrobial activities of copper complexes derived from 4-aminoantipyrine derivatives. *Journal of Saudi Chemical Society,* 17, 285-294. https://doi.org/10.1016/j.jscs.2011.04.007

Joseph, J. and Rani, G. A. B. (2014). Metal-based molecular design tuning biochemical behavior: synthesis, characterization, and biochemical studies of mixed ligand complexes derived from 4-aminoantipyrine derivatives. *Spectroscopy Letters,* 47, 86-100. https://doi.org/10.1080/00387010.2013.776087

Kedare, S. B. and Singh, R. (2011). Genesis and development of DPPH method of antioxidant assay. *Journal of food science and technology,* 48, 412-422 https://doi.org/10.1007/s13197-011-0251-1

Kortemme, T., Morozov, A. V., and Baker, D. (2003). An orientation-dependent hydrogen bonding potential improves prediction of specificity and structure for proteins and protein–protein complexes. *Journal of molecular biology*, *326*(4), 1239-1259. https://doi.org/10.1016/S0022-2836(03)00021-4

Kostova, I. and Saso, L. (2013). Advances in research of Schiff-base metal complexes as potent antioxidants. *Current medicinal chemistry,* 20, 4609-4632.
https://doi.org/10.2174/09298673113209990149

Küçükgüzel, Ş. G. and Şenkardeş, S.(2015). Recent advances in bioactive pyrazoles. *European Journal of Medicinal Chemistry,* 97, 786-815.
https://doi.org/10.1016/j.ejmech.2014.11.059

Lee, C., Yang, W. and Parr, R. G. (1988). Development of the Colle-Salvetti correlation-energy formula into a functional of the electron density. *Physical review B,* 37, 785. https://doi.org/10.1155/2014/639392

Mohamed, M., Abdelakder, H. and Abdellah, B. (2021). Microwave assisted synthesis of 4-aminophenol Schiff bases: DFT computations, QSAR/Drug-likeness proprieties and antibacterial screening. *Journal of Molecular Structure,* 1241, 130666.
https://doi.org/10.1016/j.molstruc.2021.130666

Mohanram, I. and Meshram, J. (2014). Synthesis and biological activities of 4-aminoantipyrine derivatives derived from betti-type reaction. *International Scholarly Research Notices,* 2014 (1), 639392. https://doi.org/10.1155/2014/639392

Ohkawa, H., Ohishi, N. and Yagi, K. (1979). Assay for lipid peroxides in animal tissues by thiobarbituric acid reaction. *Analytical biochemistry,* 95, 351-358.
https://doi.org/10.1016/0003-2697(79)90738-3

Ovung, A. and Bhattacharyya, J. (2021). Sulfonamide drugs: Structure, antibacterial property, toxicity, and biophysical interactions. *Biophysical reviews,* 13, 259-272. https://doi.org/10.1007/s12551-021-00795-9

Panigrahi, S. K., and Desiraju, G. R. (2007). Strong and weak hydrogen bonds in the protein–ligand interface. *Proteins: Structure, Function, and Bioinformatics*, *67*(1), 128-141.
https://doi.org/10.1002/prot.21253

Patil, R., Das, S., Stanley, A., Yadav, L., Sudhakar, A. and Varma, A. K. (2010). Optimized hydrophobic interactions and hydrogen bonding at the target-ligand interface leads the pathways of drug-designing. *PloS one*, *5*(8), e12029.
https://doi.org/10.1371/journal.pone.0012029

Ponnan, P., Gupta, S., Chopra, M., Tandon, R., Baghel, A. S., Gupta, G., Prasad, A. K., Rastogi, R. C., Bose, M. and Raj, H. G. (2013). 2D-QSAR, Docking Studies, and In Silico ADMET Prediction of Polyphenolic Acetates as Substrates for Protein Acetyltransferase

Function of Glutamine Synthetase of Mycobacterium tuberculosis. *International Scholarly Research Notices,* 2013, 373516. https://doi.org/10.1155/2013/373516

Rana, K. M., Maowa, J., Alam, A., Dey, S., Hosen, A., Hasan, I., Fujii, Y., Ozeki, Y. and Kawsar, S. M. (2021). In silico DFT study, molecular docking, and ADMET predictions of cytidine analogs with antimicrobial and anticancer properties. *In Silico Pharmacology,* 9, 1-24. https://doi.org/10.1007/s40203-021-00102-0

Reddy, G. M., Garcia, J. R., Reddy, V. H., De Andrade, A. M., Camilo Jr, A., Ribeiro, R. A. P. and De Lazaro, S. R. (2016). Synthesis, antimicrobial activity and advances in structure-activity relationships (SARs) of novel tri-substituted thiazole derivatives. *European Journal of Medicinal Chemistry,* 123, 508-513. https://doi.org/10.1016/j.ejmech.2016.07.062

Roesslein, M., Hirsch, C., Kaiser, J.-P., Krug, H. F. and Wick, P. (2013). Comparability of in vitro tests for bioactive nanoparticles: a common assay to detect reactive oxygen species as an example. *International journal of molecular sciences,* 14, 24320-24337. https://doi.org/10.3390/ijms141224320

Ruch, R. J., Cheng, S.-J. and Klaunig, J. E. (1989). Prevention of cytotoxicity and inhibition of intercellular communication by antioxidant catechins isolated from Chinese green tea. *Carcinogenesis,* 10, 1003-1008. https://doi.org/10.1093/carcin/10.6.1003

Sakthivel, A., Jeyasubramanian, K., Thangagiri, B. and Raja, J. D. (2020). Recent advances in Schiff base metal complexes derived from 4-aminoantipyrine derivatives and their potential applications. *Journal of Molecular Structure,* 1222, 128885. https://doi.org/10.1016/j.molstruc.2020.128885

Sherif, S. H., Kure, D. A., Moges, E. A. and Argaw, B. (2021). Synthesis., Characterization, and Antibacterial, Activity, Evaluation of 4-amino Antipyrine. Derivatives and Their Transition Metal Complexes. *American Journal of Bioscience and Bioengineering,* 9, 8-12. https://doi.org/10.11648/j.bio.20210901.12

Steinbach, G., Lynch, P. M., Phillips, R. K., Wallace, M. H., Hawk, E., Gordon, G. B., Wakabayashi, N., Saunders, B., Shen, Y. and Fujimura, T. (2000). The effect of celecoxib, a cyclooxygenase-2 inhibitor, in familial adenomatous polyposis. *New England Journal of Medicine,* 342, 1946-1952. https://doi.org/10.1056/NEJM200006293422603

Truhlar, D. G. " Effective Potentials for Intermediate-Energy Electron Scattering: Testing Theoretical Models," DG Truhlar, in Chemical Applications ofAtomic and Molecular Electrostatic Potentials, edited by P. Politzer and DG Truhlar (Plenum Press, New York, 1981), pp. 123-172. https://doi.org/10.1007/978-1-4757-9634-6_8

Uslaner, J. M., Parmentier-Batteur, S., Flick, R. B., Surles, N. O., Lam, J. S., Mcnaughton, C. H., Jacobson, M. A. and Hutson, P. H. (2009). Dose-dependent effect of CDPPB, themGluR5 positive allosteric modulator, on recognition memory is associated with GluR1 and CREB phosphorylation in the prefrontal cortex and hippocampus. *Neuropharmacology,* 57, 531-538. https://doi.org/10.1016/j.neuropharm.2009.07.022

Vinodkumar, C. and Radhakrishnan, P. (1997). Complexes of Yttrium and Lanthanide Perchlorates with 4-N-(2'-Thienylidene) aminoantipyrine. *Synthesis and Reactivity in Inorganic and Metal-Organic Chemistry,* 27, 1365-1372. https://doi.org/10.1080/00945719708000164

Yadav, D. K., Kumar, S., Saloni, Singh, H., Kim, M.-H., Sharma, P., Misra, S. and Khan, F. (2017). Molecular docking, QSAR and ADMET studies of withanolide analogs against breast cancer. *Drug Design, Development and Therapy*, 11, 1859-1870. https://doi.org/10.2147/DDDT.S130601